# MECHANICAL PROPERTIES OF THE FROG SARCOLEMMA

R. WAYNE FIELDS

*From the Department of Physiology, University of Oregon Medical School, Portland, Oregon 97201. Dr. Fields' present address is the Biophysics Laboratory, University of Oregon Dental School, Portland, Oregon 97201.*

ABSTRACT The elastic properties of cylindrical segments of sarcolemma were studied in single striated fibers of the frog semitendinosus muscle. All measurements were made on membranes of retraction zones, cell segments from which the sarcoplasm had retracted. Quantitative morphological studies indicated that three deforming forces interact with the intrinsic elastic properties of the sarcolemma to determine membrane configuration in retraction zone segments. The three deforming forces, namely intrazone pressure, axial fiber loads, and radial stresses introduced by retracted cell contents, could all be experimentally removed, permitting determination of the "undeformed" configuration of the sarcolemma. Analysis of these results indicated that membrane of intact fibers at rest length is about four times as wide and two-thirds as long as undeformed membrane. Membrane geometry was also studied as a function of internal hydrostatic pressure and axial loading to permit calculation of the circumferential and longitudinal tension-strain (T-S) diagrams. The sarcolemma exhibited nonlinear T-S properties concave to the tension axis in both directions. Circumferential T-S slopes (measures of membrane stiffness) ranged from 1500 to greater than 50,000 dynes/cm over the range of deformations investigated, while longitudinal T-S slopes varied from 23,000 to 225,000 dynes/cm. Thus, the membrane is anisotropic, being much stiffer in the longitudinal direction. Certain ramifications of the present results are discussed in relation to previous biomechanical studies of the sarcolemma and of other tissues.

## INTRODUCTION

The sarcolemma of striated muscle fibers is an elastic material (1–3) composed of several distinct layers (4). It is known to contribute significantly to the passive elasticity of muscle (5), although the quantitative details of the membrane's elastic responsibilities have been the subject of much debate (5–7). There has even been confusion expressed as to just what components should be included in the structure designated as the sarcolemma (8). For the present treatment, the term sarcolemma will be reserved to denote, proceeding sequentially from the membrane-sarcoplasm interface outward, the plasma membrane, the amorphous basement membrane layer, and the surrounding fibrous connective tissue investments that tend to remain in intimate association with the muscle fiber following dissection (4, 9).

The mechanical properties of the sarcolemma have been commonly investigated in portions of isolated fibers from which the cell contents have retracted following mild damage (2–4). The "retraction zone" so formed is characterized morphologically by a tubular region of membrane, supposedly containing a fluid since it has no obvious structural contents (2), and bounded at each end by coagulated sarcoplasmic debris (4). The central tube region has been described as exhibiting a curved longitudinal contour having a minimum central diameter which tapers to larger diameters near the ends (10), and thus would be classified as an anticlastic surface. The mechanical properties of retraction zone membrane are considered to be representative of those of the sarcolemma of normal muscle fibers, because the outer connective tissue investments, which are believed to be responsible for the principal rigidity of the membrane (9), are retained following retraction zone formation (4).

If the assumptions regarding retraction zone structure are correct, the morphology of the tubular segment of membrane can be described in terms of a thin elastic shell of cylindrical geometry subjected to certain external deforming forces. In the present report the nature of these external forces is investigated and the "undeformed" configuration of the membrane material, that configuration found when all external forces are zero, is established. Knowledge of the undeformed membrane geometry is uniquely important (11), because it serves as the reference state for experimental characterizations of both the bidirectional stress-strain properties of the sarcolemma and the configuration of the membrane material in the intact muscle fiber.

## MATERIALS AND METHODS

### *Isolation of Segments of Single Muscle Fibers*

The experiments were carried out on segments of single fibers isolated from the semitendinosus muscle of the frog (*Rana pipiens*). Each isolated segment was approximately one-half the length of the entire fiber. It was bounded on one end by a small piece of retained tendon and at the other terminal by a group of stumps of neighboring fibers firmly interlaced by connective tissue associated with the muscle nerve. The retained portion of tendon and fiber stumps served as convenient points of attachment to the experimental apparatus. Fiber isolation was conducted in a small dissecting chamber containing Ringer's solution (6.5 g/liter NaCl, 0.2 g/liter KCl, 0.2 g/liter $CaCl_2$, 1.0 g/liter glucose, 0.01 M phosphate to pH 7.3) at 3–5°C. Small (30 gage) syringe needles were used as knives to aid separation of individual fibers. The fiber segment was isolated from a muscle which had been removed from the frog the previous day and permitted to equilibrate overnight at 3°C in Ringer's.

### *Experimental Chamber*

An isolated fiber segment was transferred in a small cup to a separate chamber, prefilled with Ringer's solution at room temperature (22–24°C), for the performance of experiments. The experimental chamber was a rectangular plexiglass container, 10 × 15 cm in area and 1 cm deep, and was designed to allow its rigid attachment to the stage of a trinocular microscope.

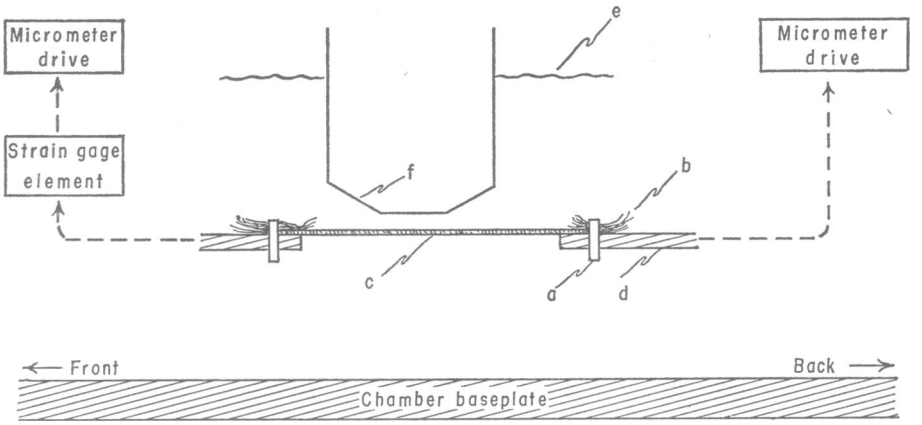


FIGURE 1 Fiber mounting apparatus in the experimental chamber. Minute rubber bands (*a*) clamp the terminal tufts (*b*) of an isolated fiber segment (*c*) to support arms (*d*). The position of the mounted fiber as it is situated during the conduct of an experiment is indicated with respect to the chamber baseplate, surface of the Ringer's solution (*e*), micrometer drive assemblies, and the objective lens of the microscope.

The isolated fiber segment was fastened between two support arms (Fig. 1) by minute rubber bands cut from tubing. In addition to providing connections for the fiber ends, the support arms also served to adjust cell length, since the position of each support along the fiber axis was controlled by an independent micrometer drive assembly connected to the baseplate of the experimental chamber. The mounting apparatus permitted the fiber segment to be horizontally supported and positioned under the microscope objective lens, with both the objective and the cell preparation submerged in Ringer's solution. One micrometer drive support assembly contained a strain gage (modified Grass model FT-03 (Grass Instrument Co., Quincy, Mass.), sensitivity 1 $\mu$v/dyne) connected to one channel of a Grass model 5 polygraph (Grass Instrument Co.) for recording the force exerted by the fiber.

The mounting apparatus was arranged to provide access of a micropipette (1.0–3.0 $\mu$ O.D.) which was also submerged in the chamber and oriented perpendicularly to the fiber and optical axes. The micropipette functioned as a mechanical probe and, following insertion through the sarcolemma, as a means of controlling the hydrostatic pressure inside the tubular sheath of retraction zone membrane. Positional control of the micropipette was accomplished with a Leitz micromanipulator (Techical Instrument Co., San Francisco, Calif.).

### *Morphological Investigations*

Usually, no morphologic derangements were apparent in the isolated fiber segments. After preliminary examination, acceptable cell preparations were damaged in a mild and controlled fashion by compression between two micropipette barrels in an attempt to induce the formation of retraction zones. The subsequent sequelae of events were permitted to develop for approximately 1 hr.

The damage formation sequence was qualitatively observed in hundreds of fibers to establish the important attributes of this phenomenon and the general morphological features of the resultant retraction zones. Certain observations important in a mechanical analysis of retraction zone membrane are described and photomicrographically documented.

The qualitative observations pointed to the necessity of developing a quantitative index of the relative shapes of empty tube membrane segments. Lengths ($L_Z$) of these regions were measured between the point at either end where membrane first made contact with clotted cell contents (averaged if necessary), while diameters of the zone membrane ($D_Z$) were determined at the site of minimum width in the central portion of the empty tube segment. The quantities $L_Z$ and $D_Z$ were normalized for interzone comparisons by dividing each value by the diameter of an undamaged portion of the same fiber (designated $D_N$). To minimize errors introduced by elliptical fiber cross-sections, the value of $D_N$ employed was an average of four to five measurements recorded before fiber damage at separated locations along the fiber segment. The resultant quantities $D_Z/D_N$ and $L_Z/D_N$ were referred to as "normalized zone shape variables." The quantities $D_Z$, $L_Z$, and $D_N$ were all measured at "reference length" of the cell preparation, defined as that length at which the passive force would rise above zero by 1 mg if the fiber segment were further extended. Only those zones that were visibly free of internal debris and fiber twist were selected for study. Furthermore, the dimensions $L_Z$ and $D_Z$ were recorded under conditions in which the hydrostatic pressure difference across the tube region membrane was at most 10 mm Hg, which is less than the pressures required to produce detectable membrane deformations (see Results).

Lengths of cell or membrane segments were recorded as divisions on an eyepiece micrometer contained in a 5× eyepiece, the accuracy of measurement being 1% of the maximum lengths encountered. Diameters were determined with a similar accuracy using an 18× eyepiece and a second micrometer disc. Both eyepiece micrometers were centered in the field of view and occupied less than half the microscopic field, thus minimizing optical aberrations. Eyepieces of different magnification were used simultaneously to permit rapid sequential measurements of the quantities over distances permitting convenience and sufficient accuracy. Both micrometer discs were calibrated against a stage micrometer submerged in Ringer's solution and viewed under identical conditions of illumination and position to those employed experimentally. The single objective lens was a Cooke-Baker 40× air lens (NA 0.7) (Cooke, Troughton and Simms Ltd., London, England) which had been waterproofed for use in Ringer's solution by applying calking material to all glued junctions.

Rarely, retraction zones of exceptional length and having a central portion of purely cylindrical (not anticlastic) geometry are formed. The presence of the cylindrical geometry was verified within experimental error by multiple measurements of zone diameter at separated points in the central tube segment. These "long" retraction zones can also be produced at will as described later. The central cylindrical portions of long retraction zones, which represent undeformed membrane under the proper conditions, were compared to intact regions of the same fiber with respect to diameters to assess the relative circumferential elongation of the sarcolemma in the normal cell.

### *Bidirectional Tension-Strain Measurements*

The lengths and diameters of central cylindrical segments of long retraction zones were measured to within 1% of their maximum values as functions of the intrazone pressure and the tensile load on the muscle fiber to permit calculation of the tension-strain behavior of the sarcolemma in both the circumferential and longitudinal directions. As in the morphological studies, extreme care was taken to select only those zones which showed no visible signs of being twisted or containing sarcoplasmic debris that might have influenced zone geometry. A sensitive test for these features was also obtained by qualitatively observing the characteristics of zone expansion in response to increasing intrazone pressure.

Zone segment lengths were recorded as the distance between marks adherent to the mem-

brane. The marks were selected from among the many bits of sarcoplasmic (inner surface) or extracellular (outer surface) debris that were visible through the microscope. In the central cylindrical region of long retraction zones it was found that marks on the inner and outer surfaces did not move with respect to one another (within experimental error) so that marks in either location would give an equally valid index of membrane length changes. The marks selected were usually on the outer membrane surface, however, which is the purported location of the elements principally responsible for membrane rigidity (9). Zone segment diameters were recorded as the distance between the center of the first diffraction band at each side of the zone (the actual membrane thickness is below the resolution of the light microscope; reference 8).

Intrazone hydrostatic pressure was controlled using a micropipette (1.0–3.0 $\mu$ O.D.) inserted through the tube membrane in the region of anticlastic geometry near one end, far removed (100–300 $\mu$) from the site of geometrical measurements. The pressures employed ranged from 0 to 10 atmospheres. Pressures were recorded in the external system communicating with the micropipette lumen by means of a Statham UGP4 pressure accessory (Statham Instruments, Inc., Oxford, Calif.) containing a UGP4-200 diaphragm (limit 13 atm.). Diaphragm distortion was sensed by a Statham UC3 universal transduction cell (Statham Instruments, Inc.) and was recorded on a second channel of the Grass polygraph used for recording the force measurements. The pressure measurements proved to be accurate within 1% of full scale and were periodically zeroed with respect to room air. Tensile force in the cell preparation was measured as previously described.

The experimental procedure was initiated by first determining the undeformed configuration of a cylindrical segment of long-zone membrane. The axial criterion for this condition occurred by definition at reference length of the cell which was determined. The micropipette was then inserted into the zone lumen, the intrazone pressure was set to zero, and the now undeformed dimensions of a selected segment of cylindrical membrane were recorded. Lengths were measured as the distance between specks of debris adherent to the membrane.

At this particular fiber length, the pressure was increased in step fashion to some positive value and recorded (within 2–4 sec) along with the diameter and length of the selected membrane segment and the tensile force (which did not change with increasing pressure at constant fiber length). After the measurements, the pressure was quickly returned to zero and a few seconds were allowed before further measurements were attempted. Measurements were rapidly recorded and the duration of pressure episodes was minimized in an attempt to reduce any viscoelastic adjustments in the membrane. The procedure was repeated for various pressures at the same fiber length until a substantial range of membrane diameters had been sampled, the procedures at a particular fiber length being referred to as a pressure run. The sequence of pressures within a run were randomized to minimize the accumulation of membrane adjustments and to provide a means of assessing measurement reproducibility. Data was similarly collected for additional pressure runs at increasing cell lengths until a membrane extension was reached at which pressure changes no longer produced measurable alterations in diameter. It was not practical to return the cell to reference length between measurements.

### *Tension-Strain Data Analysis*

Static analysis of a thin-walled cylinder under internal pressure and axial loading shows that the following relationships hold:

$$T_s = PR \qquad T_p = PR/2$$
$$T_f = F/2\pi R \qquad T_x = T_p + T_f ,$$

where $P$ is the hydrostatic pressure difference across the cylinder wall (dynes/cm$^2$), $R$ is the radius of the cylinder (cm), $F$ is the axial load on the cylinder wall (dynes), $T_s$ is the circumferential tension in the cylinder wall (dynes/cm), $T_p$ and $T_f$ are the components of longitudinal tension in the cylinder wall due to internal pressure and axial loading, respectively (both in dynes/cm), and $T_x$ is the total longitudinal tension (dynes/cm). From each measurement set, consisting of a pressure, length, diameter, and force value for a specific membrane configuration, the circumferential and longitudinal tensions were calculated, the tension in each direction being correlated with the respective membrane elongation. Membrane deformations were reported as strains (cm/cm), defined as the change in length relative to the length of undeformed membrane. Thus,

$$e_s = (S - S_0)/S_0 \qquad e_x = (X - X_0)/X_0 ,$$

where $e_s$ and $e_x$ are the circumferential and longitudinal strains, $S$ and $X$ are the measured diameter and length of the membrane under deformation, and $S_0$ and $X_0$ are the corresponding dimensions of the undeformed membrane.

## RESULTS

### *Damage Formation and Retraction Zone Morphology*

A spectacular and remarkably repeatable series of events ensues in cell segments subjected to the gentle mechanical trauma introduced for damage induction. Fig. 2 illustrates photomicrographic documentation of particular stages noted in the damage formation sequence, certain features of which have been observed by previous authors. An initially undamaged segment of an isolated fiber (Fig. 2 A) loses its characteristic cross-striations and forms two "primary clots" or regions of rigid congelated material straddling the site of damage (Fig. 2 B). Regions of disorganized muscle contents with (Fig. 2 B) or without (Fig. 2 C) local areas of coagulation can be seen to lie between and on either side of the primary clots (10, 12). The diameter of the fiber at the level of the primary clots is without exception much greater than that of normally striated portions, while the "disorganized regions" adjacent to the clots exhibit transitional diameters (Fig. 2 C).

As time progresses the disorganized regions slowly change their geometry, becoming longer and narrower. The morphologic reorganization is accompanied by further incorporation of sarcomeres adjacent to the two distally located disorganized regions, as nearby sarcomeres can be seen to be "pulled" into the growing disrupted material. Subsequently, the sarcolemma can be seen to separate from the underlying disorganized substance, the detachment beginning as a bubble (Figs. 2 D and E, 3 B), and becoming complete with the formation of an annular ring (Fig. 3 B). Finally, the reorganization culminates in division of the disrupted material, followed by retraction of the two halves of material from one another for some distance inside the remaining tubular sheath of sarcolemma. Usually, the divided disorganized material then coagulates to form rigid "plugs" identical in appearance to the primary clots formed at the initial site of damage (Fig. 4).

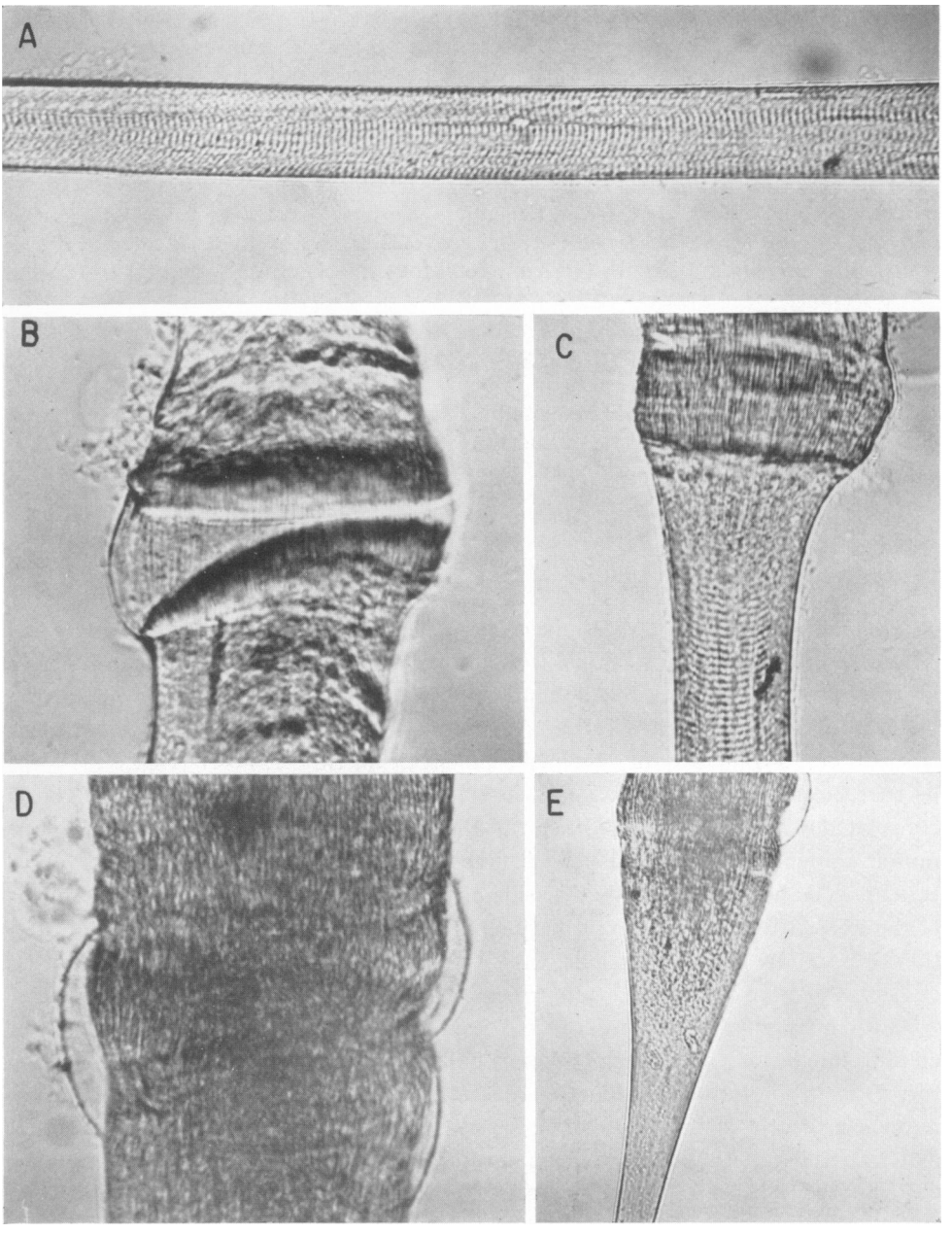


FIGURE 2 Photomicrographs of the damage formation sequence. (A) Undamaged segment of an isolated fiber. 230×. (B) Two primary clots formed at the site of damage. 345×. (C) Transition from intact fiber region to clot. 265×. (D) Membrane separation as "bubbles" from underlying disorganized material. 345×. (E) Formation of a retraction zone. 170×. Cell material of a disorganized region has just separated, leaving an empty tube region in the lower portion of the photo. The disorganized material at the top has not yet clotted. A–E, all from the same fiber.

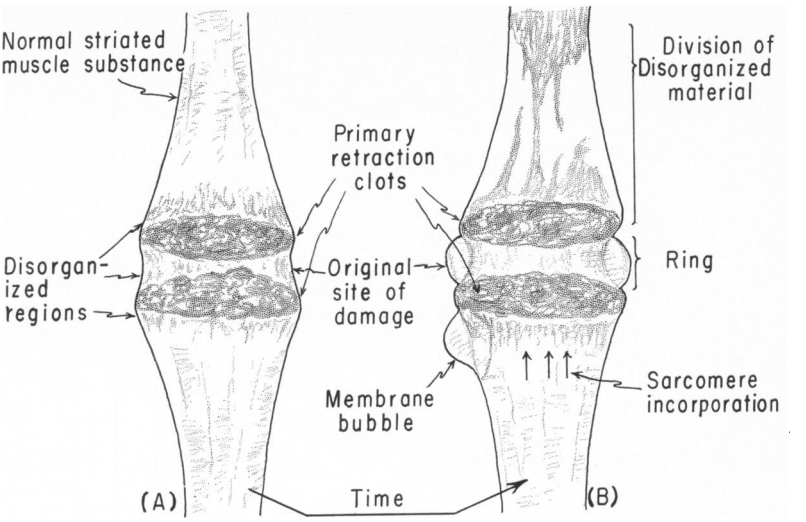


FIGURE 3 Drawings of general morphological features seen during damage development. (A) Two primary clots straddling the site of damage with three associated regions of disorganized muscle contents. Any one of the three disorganized regions can potentially form a retraction zone. (B) Transformation of disorganized regions is illustrated chronologically from below. Lower region shows formation of membrane bubble which eventually becomes an annular ring as illustrated in the central region. The upper disorganized region is depicted during division, the outwardly bulging ring membrane inverting its longitudinal contour as separation becomes complete.

Fig. 4 is a diagram of general retraction zone morphology, characterized by a central empty tube region bordered sequentially on either end by clots and regions of disorganized striation. The central "tube" region exhibits a curved longitudinal contour with minimum diameter near the center, the change in curvature with length being most accentuated near the clots. The tube region supposedly contains a fluid (2), relegating the support of longitudinal and lateral loadings to the membrane within this segment of the muscle fiber. The fluid nature of the zone interior is further substantiated in a later section.

The latter model is confirmed by experimental observations associated with the present work. The cross-sectional outline of the tube, observed by rotating the fiber with a micropipette, may be grossly elliptical near the ends as dictated by the shape of the clots, but is circular in the center if the retraction zone is of sufficient length. The clots are of irregular shape and have diameters ranging from 25–250% of that found in the undamaged fiber, although the smaller diameters are found only in clots formed secondary to division of the disorganized material. It is significant that the tube region membrane always tapers to a smaller central diameter even when associated with the smallest clots observed. In addition, subsequent discussion will establish that membrane geometry is uniquely determined by intrazone pressure under conditions of constant muscle fiber environment and axial loading. Further-

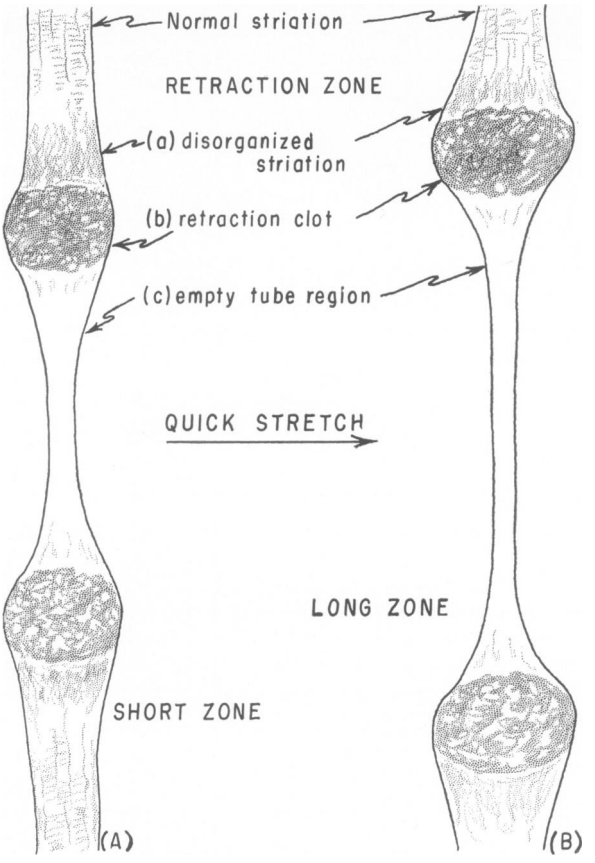


FIGURE 4 Structural details of retraction zones in general and of the "short" versus "long" zone morphological classes. The tube regions of short zones show curvilinear contour (anticlastic geometry) throughout their length, while long zones are distinguished by having a central tube segment of cylindrical geometry.

more, membrane encompassing a clot tends to mold itself over irregularities with curvilinear indentations, and to reversibly form a sharp conical indentation when nudged with a micropipette. Such behavior suggests that the retraction zone represents a fluid-filled cylindrical segment of elastic membrane which is being stretched circumferentially by the swollen clotted material plugging each end, the induced radial distortions progressively decaying toward the center of the tube region.

Retraction zones form at variable lengths, depending on how far the divided halves of disorganized material retract after separation. Two morphological classes of retraction zones can be distinguished, designated with respect to relative length as "short" and "long" zones (Fig. 4). Short zones exhibit a curvilinear longitudinal contour throughout the tube region, whereas long zones have a central tube segment of purely cylindrical geometry, with a curvilinear outline (anticlastic geometry)

found only near the clots. The two zone classes are identical in all other morphological features, and it appears that the cylindrical portion of long zones is merely a membrane region far enough removed from the clots to be free of associated geometrical distortions ("end effects").

*Circumferential Strain of the Sarcolemma in Intact Fibers*

The observed short-long zone length distinction has important mechanical implications. In mechanics, configurations of a thin[1] elastic structure are usually referred to the dimensions of the material in its undeformed state, found when all deforming forces are zero (13). Analysis of retraction zone morphology, considering the sarcolemma as a thin elastic cylindrical shell under internal pressure and various external loadings, indicates that all deforming forces in a segment of tube membrane can be removed if the intrazone pressure and the force on the muscle fiber are experimentally fixed at zero and the membrane portion under consideration is restricted to the central cylindrical region of a long retraction zone.

The preceding considerations are quantitatively demonstrated by a plot of the relative zone shape variables, $D_Z/D_N$ and $L_Z/D_N$, determined in 39 different zones at various zone lengths (Fig. 5). These measurements were recorded at reference length of the fiber and zero intrazone pressure, and therefore represent conditions in

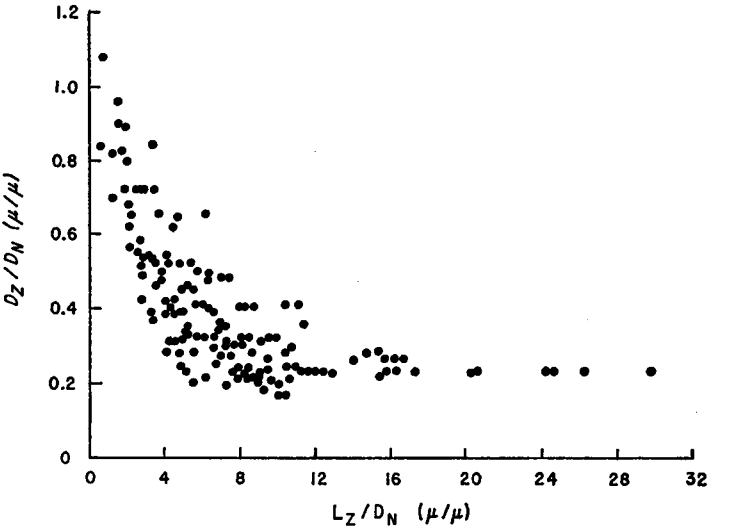


FIGURE 5 Graphical representation of "normalized zone shape variable" data. Each point represents the central (minimum) diameter ($D_Z$) and length ($L_Z$) of a retraction zone tube region, after both dimensions were divided by the diameter of an intact region of the same fiber ($D_N$). All measurements were recorded at reference length of the cell and with the intrazone hydrostatic pressure equal to zero.

[1] According to Kraus (13), a shell can be considered to be thin if the radii of curvature at the particular point exceed the shell thickness by a factor of at least 10.

TABLE I

NORMALIZED ZONE DIAMETERS ($D_Z/D_N$) FOR RETRACTION ZONES OF THE "LONG" MORPHOLOGICAL CLASS

| Number | $D_N$ | $D_Z$ | $L_Z$ | $D_Z/D_N$ |
|---|---|---|---|---|
| | $\mu$ | $\mu$ | $\mu$ | $\mu/\mu$ |
| 1 | 45 | 10 | 405 | 0.22 |
| 2 | 67 | 14 | 560 | 0.21 |
| 3 | 39 | 9 | 366 | 0.23 |
| 4 | 39 | 9 | 637 | 0.23 |
| 5 | 76 | 15 | 675 | 0.20 |
| 6 | 76 | 17 | 1,178 | 0.22 |
| 7 | 76 | 16 | 733 | 0.21 |
| 8 | 79 | 15 | 801 | 0.19 |
| 9 | 77 | 18 | 868 | 0.23 |
| 10 | 58 | 15 | 810 | 0.26 |
| 11 | 71 | 15 | 618 | 0.21 |
| 12 | 74 | 18 | 782 | 0.24 |
| 13 | 78 | 16 | 627 | 0.21 |
| 14 | 74 | 21 | 1,527 | 0.28 |
| 15 | 113 | 18 | 1,158 | 0.16 |

The indicated value of $L_Z$ represents the shortest length at which the long-zone morphology was observed. Since the measurements followed a quick-stretch episode, the values are in general an overestimate of the minimum zone length at which the long-zone morphology would be manifest.

which the only membrane deforming force of possible consequence is that related to end effects. For short zone lengths, the relative diameter $D_Z/D_N$ decreases with increasing relative zone length $L_Z/D_N$, reflecting the decay of end effect distortions in the center of the tube region membrane as this region becomes farther removed from the clots. Eventually, a state is reached where $D_Z/D_N$ becomes independent of further increases in relative zone length, this relationship being a quantitative representation of the long zone morphology.

Short zones were routinely converted into zones of longer relative shape by subjecting the fiber preparation to quick-stretch episodes (50% increase in fiber segment length in 1 sec). This procedure does not result in membrane breakdown or reorganization. Observations of the relative positions of membrane marks before and after quick-stretch episodes indicated that the sarcolemma is free to move with respect to underlying disrupted cell contents, longer zones arising by further retraction of the clots. The observed marks were located on both inner and outer membrane aspects.

In many experiments, it was possible to obtain repetitive measurements of zone shape variables from the same zone in both the short and long morphological configurations. The final values of $D_Z/D_N$ found for long zones of this group were remarkably constant, being 0.22 $\mu/\mu$ $\pm$0.03 $\mu/\mu$ SD ($N$ = 15). The data are sum-

marized in Table I. Once the long zone configuration has been obtained in an individual tube region ($L_Z \approx 400$ $\mu$ from Fig. 5 with $\overline{D}_N = 70$), further increases in length of up to 1100 $\mu$ cause no changes in relative diameter. The latter observation is clearly illustrated in the results of one particular zone studied. This zone was first observed in the short-zone morphology, at a length of 160 $\mu$, and was unusual in that it was spontaneously increasing in length. The growth was occurring from one end only, as tube membrane was stationary with respect to one clot, but was sliding smoothly over the other into the zone from positions overlying normal striated muscle substance. As growth continued, the long-zone morphology developed at a length of approximately 370 $\mu$. Growth continued at a uniform rate to a length in excess of 1100 $\mu$ at which time the process ceased. No changes in the measured value of $D_Z/D_N$ were detected after the long-zone configuration of tube membrane had been established.

*Directional Dependence of Membrane Tension-Strain Behavior*

The geometry (length and diameter) of central cylindrical segments of long retraction zones was studied as a function of axial loading of the muscle fiber and intrazone pressure to establish the tension-strain behavior of the sarcolemma in both the circumferential and longitudinal directions. The resulting pressure-tension–deformation data were summarized in the form of tension-strain (T-S) plots (Fig. 6). The T-S data for the circumferential direction (Fig. 6 A and C) were plotted as a family of curves for particular values of strain in the longitudinal direction. T-S data for the longitudinal direction were summarized in an analogous manner (Fig. 6 B and D). The data from each retraction zone were treated independently, Fig. 6 representing two examples out of twenty-two experiments in which intrazone pressure control was accomplished.

Several aspects of the results illustrated in Fig. 6 deserve specific emphasis. The tension-strain behavior of the membrane is markedly nonlinear, being concave to the tension axis in both coordinate directions. Furthermore, for similar tension increments, the observed range of circumferential strains greatly exceeds the range of longitudinal strains. This result indicates that the membrane material is very definitely anisotropic, being much stiffer in the longitudinal direction. Finally, referring to the circumferential T-S plots as examples and extrapolating the linear portions of each curve to the strain axis, it can be seen that the nonlinearity of the T-S curve is removed at a lower value of circumferential strain as the longitudinal strain is increased. Analogous behavior is found in the longitudinal direction, and these results are typical of all membrane segments investigated.

The tension-strain results are further summarized in the form of tension-strain slopes (T-S slopes), infinitesimal ($\Delta$ tension/$\Delta$ strain) ratios at specified values of circumferential and longitudinal strain, for both principal directions in the membrane. The marked nonlinearity of T-S relationships and the interaction between

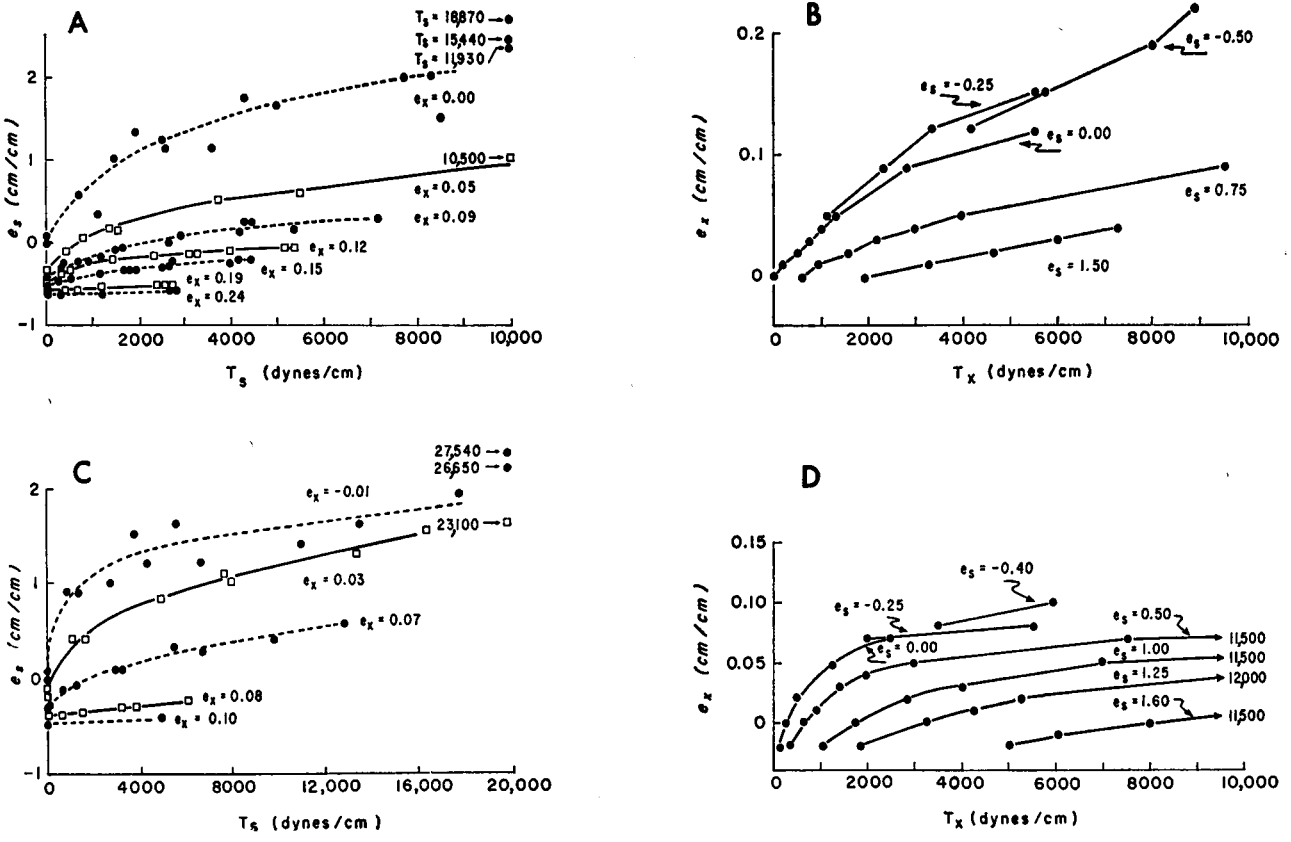


EIGURE 6 Circumferential and longitudinal tension-strain plots for the membranes studied in experiments 3 (A, B) and 5 (C, D). The experiment numbers correspond to those of Tables II and III.

TABLE II

CIRCUMFERENTIAL T-S SLOPES (DYNES/CM) AS A FUNCTION OF CIRCUMFERENTIAL TENSION ($T_s$) AT CONSTANT LONGITUDINAL STRAIN ($e_x$), AND AS A FUNCTION OF LONGITUDINAL STRAIN AT CONSTANT CIRCUMFERENTIAL TENSION

| Experiment number | $e_x$ (cm/cm) | Low | | | Moderate | High |
|---|---|---|---|---|---|---|
| | | | $T_s$ (dynes/cm) | | | |
| | 1,000 | 5,000 | 9,000 | 1,000 | 5,000 | 1,000 |
| 1 (9) | 4,000 | 11,000 | — | — | — | 32,000 |
| 2 | 5,500 | 10,500 | 20,500 | 15,000 | 23,000 | >50,000 |
| 3 (11) | 2,000 | 7,500 | 12,500 | 6,500 | 21,000 | 32,000 |
| 4 (14) | 2,000 | 8,700 | 12,000 | 14,500 | 38,000 | — |
| 5 | 2,700 | 18,000 | 34,000 | 8,500 | 21,000 | >50,000 |
| 6 (15) | 2,600 | 16,500 | 30,000 | 16,500 | 34,000 | >50,000 |
| 7 | 1,500 | 14,000 | 26,000 | 7,000 | 21,000 | 36,000 |

Experiment numbers in parentheses indicate the number of the same fiber in Table I.

TABLE III

LONGITUDINAL T-S SLOPES (DYNES/CM) AS A FUNCTION OF LONGITUDINAL TENSION ($T_x$) AT CONSTANT CIRCUMFERENTIAL STRAIN ($e_s$), AND AS A FUNCTION OF CIRCUMFERENTIAL STRAIN AT CONSTANT LONGITUDINAL TENSION

| Experiment number | $e_s$ (cm/cm) Low (−0.25) | | Moderate (0.00) | | High (0.50) | |
|---|---|---|---|---|---|---|
| | | | $T_x$ (dynes/cm) | | | |
| | <2,000 | >2,000 | <2,000 | >2,000 | <2,000 | >2,000 |
| 1 (9) | 28,000 | 164,000 | 16,000 | 116,000 | 41,000 | 100,000 |
| 2 | 26,000 | 88,000 | 18,000 | 83,000 | 61,000 | 122,000 |
| 3 (11) | 30,000 | 75,000 | 20,000 | 91,000 | 33,000 | 138,000 |
| 4 (14) | — | 68,000 | 6,000 | 60,000 | 21,000 | 158,000 |
| 5 | — | 226,000 | 9,000 | — | 14,000 | 225,000 |
| 6 (15) | 47,000 | 122,000 | 41,000 | 180,000 | 45,000 | 150,000 |
| 7 | 23,000 | 60,000 | 33,000 | 50,000 | 51,000 | 205,000 |

Experiment numbers in parentheses indicate the number of the same fiber in Table I.

tensions and strains in the two directions requires computation of T-S slopes for a series of specified conditions (Tables II and III). Longitudinal T-S slopes (Table III) are computed at "low," "moderate," and "high" circumferential strains, being −0.25, 0.00, and 0.50 cm/cm, respectively. Circumferential T-S slopes (Table II) are similarly reported for "low," "moderate," and "high" longitudinal strains. High longitudinal strain refers to values at which circumferential strains changed only slightly under maximum circumferential tension; these values varied for different experiments over the range 0.12 to 0.20 cm/cm. The low longitudinal strain specification refers to near zero values, and the moderate designation refers to strains approximately midway between the low- and high-strain quantities used in the

analysis of that particular experiment. At each specified elongation, the T-S slopes were grouped according to the tension at which they were measured. Estimates of T-S slopes involved interpolation of graphical data, and reliable estimates of a sufficient number of values could be obtained in only seven experiments.

The results of Table II indicate that circumferential T-S slopes increase (the membrane becomes "stiffer") with increasing circumferential tension ($T_s$) at constant longitudinal strain ($e_x$), and also increase with increasing longitudinal strain at constant circumferential tension. Thus, for a given membrane configuration, attempting to increase membrane dimensions either circumferentially by applying circumferential tension or longitudinally by increasing the longitudinal strain results in increased membrane "stiffness" in the circumferential direction. A similar analysis applied to the data of Table III shows that the membrane stiffness in the longitudinal direction is also increased in most instances by increasing either membrane dimension. In situations where high strains are present in both directions, circumferential T-S slopes tend to approach values found for the longitudinal direction. The marked anisotropicity seen in membrane stiffness under low deformations is largely negated when high strains are manifest in the membrane material.

### *Transzone Pressure and Micropipette Radius*

Due to the high pressures employed in the present study, it is possible that fluid leakage may occur from the retraction zones, either through the membrane in general or at the site of micropipette penetration or both. The maintenance of a stable membrane geometry (which was observed) would then require fluid to continually enter through the micropipette tip, and the pressure as recorded in the external system might not be representative of intrazone pressure. The extent of leakage could be estimated using a dye, but such information is not sufficient. Even if leakage occurs, the external pressure recording would only be in error if a significant proportion of the total resistance to fluid flow existed in the tip of the micropipette. That this is not the case is suggested by the fact that the data of Tables II and III were collected using pipettes of inside diameters estimated to be 0.5–2.0 $\mu$, or having flow resistances differing by a factor of 256, i.e., $4^4$. A significant error due to pipette tip flow resistance should result in T-S slopes differing by orders of magnitude between fibers, which is obviously not the case.

## DISCUSSION

Retraction zone formations have provided a popular preparation for investigating the mechanical properties of the sarcolemma free from structural support of intracellular elements. Basically, the procedure has been to compare elongations of zone membrane with either undamaged portions of the same fiber or with over-all cell length in an attempt to assess the relative contribution of the sarcolemma to cell extensional elasticity. Using this argument, several workers have concluded that for

short fiber lengths the elastic contributions of the sarcolemma are secondary to those of the cell contents, while at longer cell lengths (high passive tensions), the relative extensional resistance of the membrane becomes prominent (1, 7, 10). Recent evidence arising from a variety of other experimental approaches also tends to favor this viewpoint (14–16). In contrast, Ramsey and Street (2) found that the sarcolemma bears the entire brunt of passive loads at all fiber lengths.

Several critical assumptions are inherent in the above studies. It is tacitly assumed without experimental verification that the zone tube region contains a fluid so that all axial loads are borne solely by the membrane. This assumption is substantiated by the pressure deformation studies in the present work. The conclusions also require that zone and normal fiber membrane represent the same structure, which is supported by electron micrographs of normal and zone segment membranes (4), and the morphological observations showing that the sarcolemma appears to gently detach from disorganized cell contents and move freely with respect to underlying material during retraction zone formation. Lastly, it is assumed that membrane segments in normal and zone regions are in comparable stress-strain states in both the circumferential and longitudinal directions through the membrane material. The latter requirement is definitely violated as will be presently shown.

The ratio of long-zone to normal fiber diameters at reference length of the cell was found to be 0.22 $\mu/\mu$ $\pm$0.03 $\mu/\mu$ SD ($N$ = 15). These results establish the remarkable conclusion that at comparable states of longitudinal tension in the cell, the sarcolemma of intact fiber segments is elongated circumferentially by 450% (1/0.22) with respect to its diameter in the undeformed configuration. Buchthal (3) finds a longitudinal elongation of 50–70% for the emptied sarcolemma in an unloaded state compared with a corresponding portion of the intact fiber before damage. The latter finding may be quantitatively inaccurate because of neglected considerations of the scalloped longitudinal contour of the sarcolemma in intact fibers (17) and of the short-long distinction of zone morphology, but Buchthal's measurements qualitatively demonstrate that the sarcolemma is longitudinally shortened in the intact cell. Combining the above considerations, the sarcolemma in the intact cell at reference length has 450% the circumference, is 60% as long, and therefore has a surface area of about 270% of the corresponding membrane in the undeformed configuration. A complete description of the physiological role of the sarcolemma must explain the rather unusual configuration of this structure in terms of its mechanical properties and molecular composition.

As described in the Introduction, the sarcolemma is composed of a multilayered complex (4), the principal strength of which is presumably due to the outer collagen fiber investments (9). The results of the bidirectional tension-strain characterization of the sarcolemma reported in the present work are consistent with this historical viewpoint. The maximum values for tension-strain slopes of 1.0–2.2 $\times$ $10^5$ dynes/cm found for high degrees of strain in the membrane, when divided by membrane thickness ($10^{-5}$ cm) (8) to convert these T-S slopes to units of stress per unit strain,

are in excellent agreement with the published value for collagen of $1.2 \times 10^{10}$ dynes/cm$^2$ (18).

Assuming that the principal rigidity of the sarcolemma is in fact due to collagen fibril layers, it is interesting to examine various architectural arrangements of such fibrils for compatibility with the observed mechanical properties of the membrane. Previous authors have described electron micrographic evidence suggesting a helical arrangement of membrane collagen fibrils (19, 20). The nonlinear tension-strain behavior found for the sarcolemma is typical of many biological tissues (11), and has been attributed to the progressive removal of slack in collagen fibril components as tissue area is increased for the particular cases of the skin (21) and walls of arteries (22). As described elsewhere (23–25), it can be shown that the observed elastic behavior of the sarcolemma can be similarly explained in terms of an enveloping system of collagen fibrils, the full and linear elastic properties of the collagenous elements only becoming apparent under high degrees of membrane strain in which initial fibril slack has been removed. The suggested ultrastructural basis for the mechanical properties of the sarcolemma requires a spring-like helical arrangement of collagen fibrils, and quantitatively predicts a relationship between the angular pitch of the helical system and muscle fiber length. It appears that a reinvestigation of the sarcolemma in the electron microscope may be warranted, with emphasis upon studying the general arrangement of the collagen fibrils as a function of muscle fiber length.

Sincere thanks are extended to Dr. J. J. Faber for his advice and assistance during the formulation and conduct of this study.

This work was supported by PHS Grant GM 00538.

*Received for publication 11 June 1969 and in revised form 31 October 1969.*

## REFERENCES

1. SICHEL, F. J. M. 1941. *Amer. J. Physiol.* **133**:446P.
2. RAMSEY, R. W., and S. F. STREET. 1940. *J. Cell. Comp. Physiol.* **15**:11.
3. BUCHTHAL, F. 1942. *Kgl. Dan. Vidensk. Selsk. Biol. Medd.* **17**:1.
4. MAURO, A., and W. R. ADAMS. 1961. *J. Biophys. Biochem. Cytol.* **10**:177.
5. ABBOTT, B. C., and A. J. BRADY. 1964. Physiology of the Amphibia. J. A. Moore, editor. Academic Press, Inc., New York. 329.
6. MAURO, A., and O. STEN-KNUDSEN. 1952. Acta Med. Scand. Suppl. 266 **142**:715.
7. BUCHTHAL, F., and P. ROSENFALCK, 1957. Tissue Elasticity. J. W. Remington, editor. American Physiological Society, Washington, D.C. 73.
8. BARER, R. 1948. *Biol. Rev. Cambridge Phil. Soc.* **23**:159.
9. STREET, S. F., and R. W. RAMSEY. 1965. *Science* (Washington). **149**:1379.
10. CASELLA, C. 1951. *Acta Physiol. Scand.* **21**:380.
11. FUNG, Y-C. B. 1968. *Appl. Mech. Rev.* **21**:1.
12. SPEIDEL, C. C. 1939. *Amer. J. Anat.* **65**:471.
13. KRAUS, H. 1967. Thin Elastic Shells. John Wiley and Sons, Inc., New York.
14. HILL, A. V. 1952. *Proc. Roy. Soc. Ser. B. Biol. Sci.* **139**:464.
15. NATORI, R. 1954. *Jikeikai Med. J.* **1**:119.

16. GONZALEZ-SERRATOS, H. 1966. *J. Physiol. (London).* **185**:20P.
17. STREET, S. F., M. N. SHERIDAN, and R. W. RAMSEY. 1966. *Med. Coll. Va. Quart.* **2**:90.
18. CURREY, J. D. 1963. *Biorheology.* **2**:1.
19. REED, R., and K. M. RUDALL. 1948. *Biochim. Biophys. Acta.* **2**:19.
20. DRAPER, M. H., and A. J. HODGE. 1949. *Aust. J. Exp. Biol. Med. Sci.* **27**:465.
21. RIDGE, M. D., and V. WRIGHT. 1966. *J. Appl. Physiol.* **21**:1602.
22. ROACH, M. R., and A. C. BURTON. 1957. *Can. J. Biochem. Physiol.* **35**:681.
23. FIELDS, R. W. 1969. An Elastic Characterization of the Muscle Cell Membrane and its Structural Interpretation. Doctoral Thesis. University of Oregon Medical School, Portland.
24. FIELDS, R. W., and J. J. FABER. 1969. *Physiologist.* **12**:225.
25. FIELDS, R. W., and J. J. FABER. 1970. *Can. J. Physiol. Pharmacol.* In press.